World Journal of Advanced Research and Reviews

eISSN: 2581-9615 CODEN (USA): WJARAI

Cross Ref DOI: 10.30574/wjarr

Journal homepage: https://wjarr.com/

(Research Article)

Check for updates

Physico-chemical characterization of activated carbons from local lignocellulosic biomass (Niger)

Ousmaila SANDA MAMANE [1, 2], Rabilou SOULEY MOUSSA [2], Mahamane Nassirou AMADOU KIARI [2, 3, 4, *], Maâzou SIRAGI DOUNOUNOU BOUKARI [2], Ali SANDA BAWA [1], Maman Mousbahou MALAM ALMA [2] and Ibrahim NATATOU [1, 2]

[1] National School of Engineering and Energy Sciences, University of Agadez, B.P: 199 Agadez, Niger.

[2] Department of Chemistry, Faculty of Science and Technology, Materials/ Water and Environment Laboratory/ Abdou Moumouni University, B. P: 10662 Niamey, Niger.

[3] Laboratory of Industrial Processes of Synthesis, the Environment and New Energies, Institut National Polytechnique Félix Houphouët-Boigny, BP 1093, Yamoussoukro, Côte d'Ivoire.

[4] African Center of Excellence for the Recovery of Waste into High Value-Added Products, Yamoussoukro, Côte d'Ivoire.

World Journal of Advanced Research and Reviews, 2025, 27(03), 130-144

Publication history: Received on 17 July 2025; revised on 23 August; accepted on 26 August 2025

Article DOI: https://doi.org/10.30574/wjarr.2025.27.3.3054

Abstract

This study presents the physico-chemical characterization of activated carbons produced from local lignocellulosic biomass, notably the core shells of *Balanites aegyptiaca* (L.) Del. (Adoua), and *Hyphaene thebaica* (L.) Mart. (Gorouba) by chemical activation with orthophosphoric acid (H_3PO_4). Elaborated Activated Carbons (EACs) were characterized using experimental techniques such as: X-ray Diffraction using a Shimadzu XRD-6000 diffractometer, Infra-Red (IR-TF) using a spectrometer (Bruker Vector-22 Fourier transform spectrometer; ATR-FTIR), SEM using a Hitachi device at 20 kV and Raman spectroscopy. The results of this study show that Elaborated Activated Carbons did not detect any detectable crystallized species on the surface; the existence of several types of pore types (micropores, mesopores and macropores) of pores. Elaborated activated carbons have developed functional groups (carboxylic hydroxyls (O-H), asymmetrical and symmetrical C-H, C=C alkene, C=O carbonyl, C-O and C-C alkene, aliphatic and aromatic); cumulative pore volumes (BJH) vary from 0.269688 to 0.560185 $cm^3\ g^{-1}$; CAEs are capable of adsorbing molecules of micropore, mesopore and macropore sizes.

Keywords: Biomass; *Balanites aegyptiaca*; *Hyphaene thebaica*; Activated carbon; Characterization

1. Introduction

As one of the extraction methods of choice, adsorption is the most widely used technique due to its efficiency, ease of implementation and affordable investment cost [1,2, 3]. However, this method requires the choice of an adsorbent with good characteristics (high adsorption capacity, availability, low cost, etc.) [4,5]. Microporous adsorbents are widely used for the extraction of chemical species from aqueous or gaseous phases, thanks to their excellent adsorption capacity [2,5-6]. This capacity is linked to the high specific surface area and porosity development of these adsorbents [7-9]. The use of activated carbon (AC) as an adsorbent is of interest in the treatment of industrial wastewater [10,11]. Activated carbon is essentially a carbonaceous material with a porous structure. This structure is generally obtained after high-temperature carbonization of lignocellulosic biomass. Various types of AC exist, with specific surface areas ranging from 100 to 2,500 $m^2\ g^{-1}$ [12,13]. Despite the availability of biomass in the sub-region, African countries continue to import activated carbons (ACs) in large quantities for a variety of applications, including industrial wastewater treatment and ore processing. This is why it seems necessary to develop and characterize ACs from local lignocellulosic biomasses, in

* Corresponding author: Mahamane Nassirou AMADOU KIARI

particular the core shells of *Balanites aegyptiaca* (L.) Del. (Adoua), and *Hyphaene thebaica* (L.) Mart. (Gorouba) by chemical activation. The selected biomasses come from wild trees that are widespread in Niger and produce seasonal fruits consumed by the population. The pits of these fruits end up in the municipal landfill as urban waste. They constitute abundant agri-food waste that is more or less difficult to biodegrade in tropical countries. The use of these cores in this work has a dual advantage: on the one hand, to produce activated carbons, and on the other, to add value to the waste. Elaborated activated carbons (CAEs) were characterized using experimental techniques such as XRD, IR, SEM and Raman spectroscopy.

2. Materials and methods

2.1. X-Ray Diffraction (XRD)

XRD is a surface analysis technique used to determine the nature of crystalline species present on the surface of materials. For activated carbon samples, analysis was carried out using a Shimadzu XRD-6000 diffractometer equipped with a copper anode Kα radiation (λ = 0. 15418 nm; 40 kV and 30 Ma kV. These analyses were carried out at the State Key Laboratory of Chemical Engineering, Beijing University of Chemical Technology, People's Republic of China.

2.2. Fourier Transform Infrared Spectroscopy (FT-IR)

FT-IR is based on the absorption of infrared radiation by the material being analyzed. By detecting the characteristic vibrations of chemical bonds, it enables qualitative analysis of the chemical functions present in CA. The spectrum of CA was recorded at room temperature in total reflection mode using a spectrometer (Bruker Vector-22 Fourier transform spectrometer; ATR-FTIR) in the wave number range 400 to 4000 cm^{-1}. These analyses were carried out at the State Key Laborotary of Chemical Ressource Engineering of Beijing University of Chemical Technology in the People's Republic of China.

2.3. Scanning Electron Microscopy (SEM)

SEM is used to describe the morphology of Elaborated Activated Carbon. In these studies, observations were made using a 20 kV Hitachi instrument. These analyses were carried out at the State Key Laborotary of Chemical Ressource Engineering of Beijing University of Chemical Technology in the People's Republic of China.

2.4. Raman microscopy

This technique complements XRD. It is a method for observing and characterizing the molecular composition and external structure of a material. In these studies, Raman spectra were recorded at room temperature with a Microscopic Confocal spectrometer (Jobin Yvon Horiba HR800), using an Ar+ laser as the excitation source at a wavelength of 532 nm. These analyses were carried out at the State Key Laborotary of Chemical Ressource Engineering of Beijing University of Chemical Technology in the People's Republic of China.

2.5. Determining the porosity of CAEs

The surface and volume distributions of CAEs are determined by the Density Functional Theory (DFT) and BJH methods [13].

3. Results

3.1. X-ray diffraction analysis

Figure 1 shows diffractograms of activated carbons made from *Balanites aegyptiaca* (L.) Del activated with 30 % and 40 % ortho-phosphoric acid.

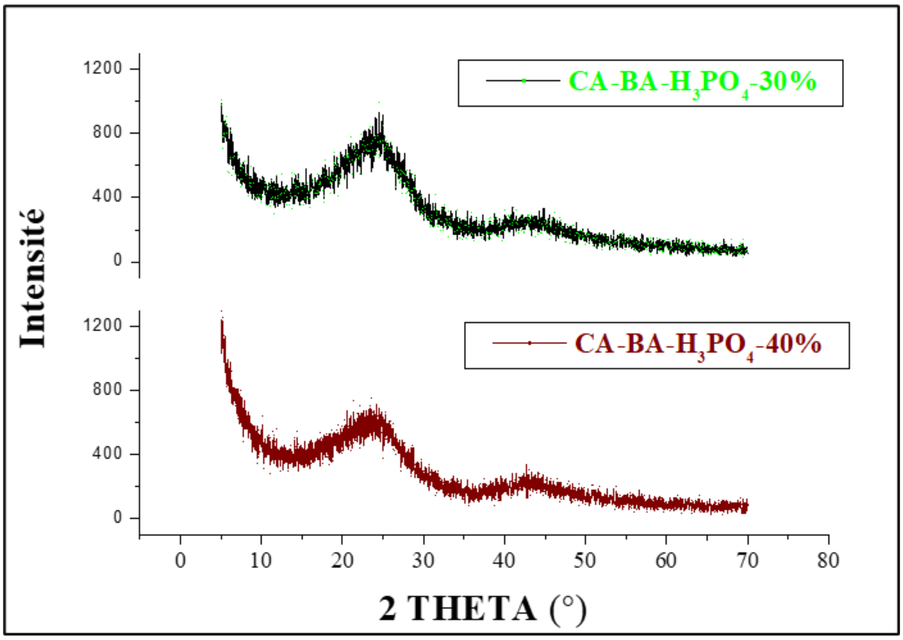

Figure 1 Diffractograms of CAEs

3.2. Analysis by infrared spectroscopy

The infrared (IR) spectra of activated carbons made from *Balanites aegyptiaca* (L.) Del activated with 30 % and 40 % ortho-phosphoric acid are shown in Figures 2 and 3.

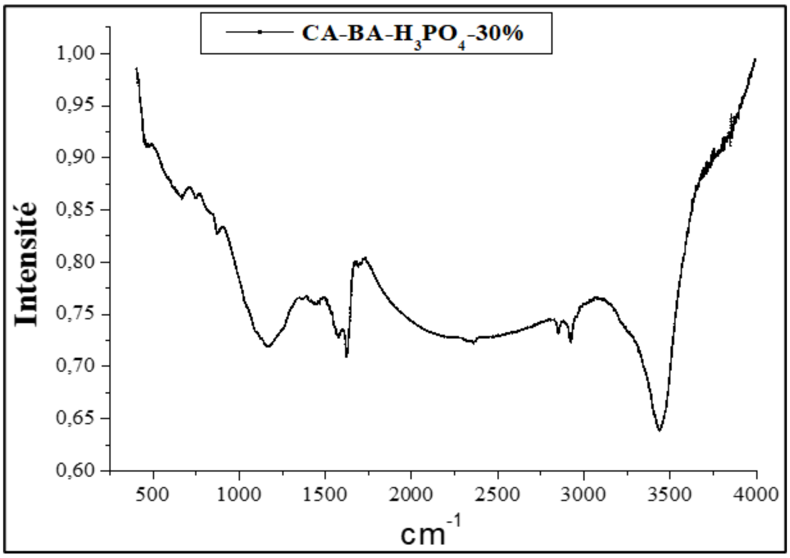

Figure 2 Infrared spectrum of CA-30 %

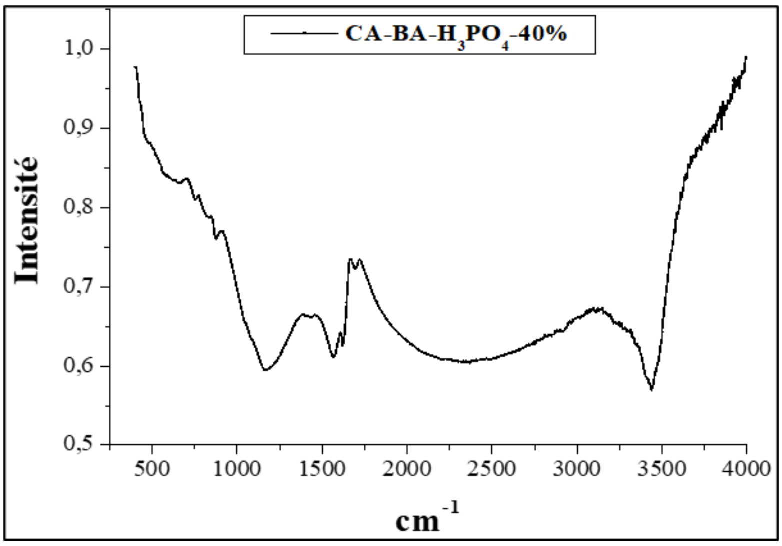

Figure 3 Infrared spectrum of CA-40 %

Analysis of the infrared spectrum of activated carbons has enabled us to identify the main signals [15-17] (Table 1).

Table 1 CAE functional groupings

Wave number (cm^{-1})			**Vibration frequency assignment**
Type	**CA-30 %**	**CA-40 %**	
Peaks	3438	3444	Carboxylated hydroxyls (O-H)
Signals	2923-2853	2918	Assymmetrical and symmetrical C-H
Bands	2800 and1735	2862 and 1731	C=C groups
Signals	1701	1702	C=O groups
Potato	1493 and 1321	-	C-O groups
Peak	1164.05	1189.46	C-C (alkene, aliphatic and aromatic)

3.3. Scanning electron microscopy analysis

In order to visualize the external morphology of CAEs, scanning electron microscopy was performed on 40 % *Balanites aegyptiaca* CA in order to see the effect of activation. Figure 4 shows the CAE images.

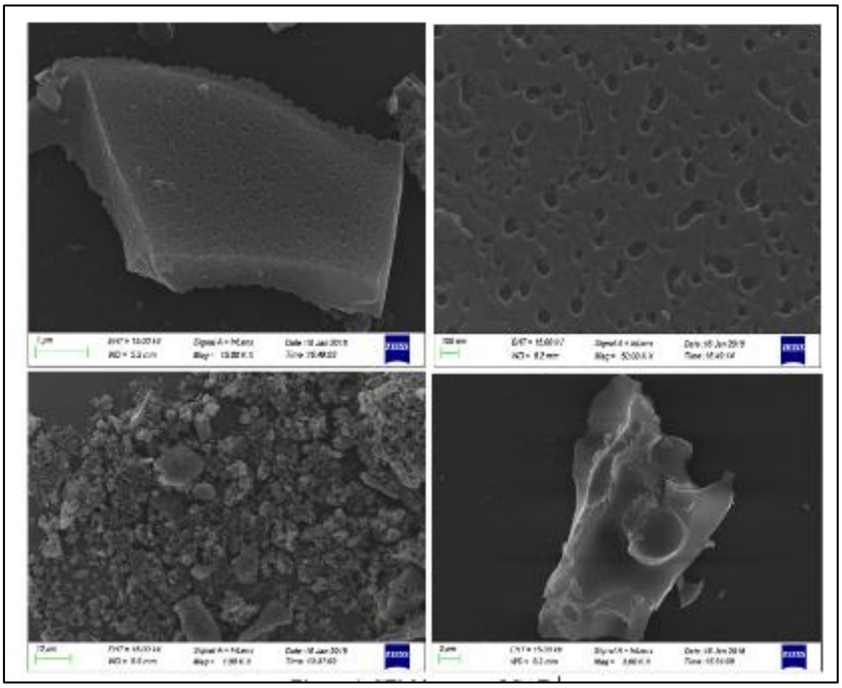

Figure 4 SEM images of CAEs

3.4. DFT pore volume distributions

Figure 5 shows the isotherms of the CAE volume distributions and the CAC.

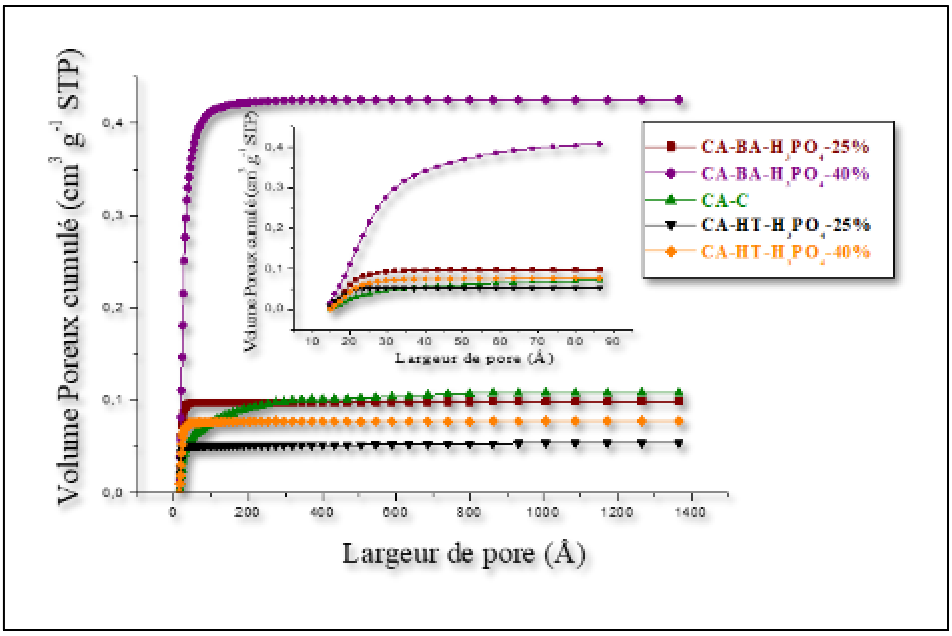

Figure 5 Volume distributions of CAEs and CA-C

Figures 6, 7, 8, 9 and 10 show the derivatives of the volume distributions of the CAEs and the CAC.

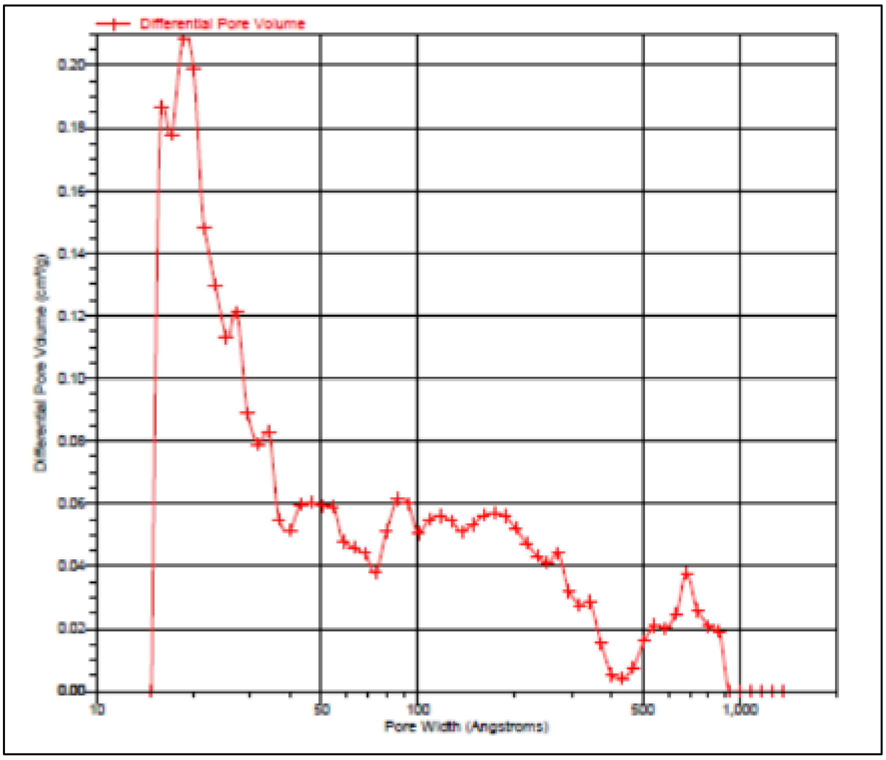

Figure 6 CA-BA-H_3PO_4-25 % volume derivative

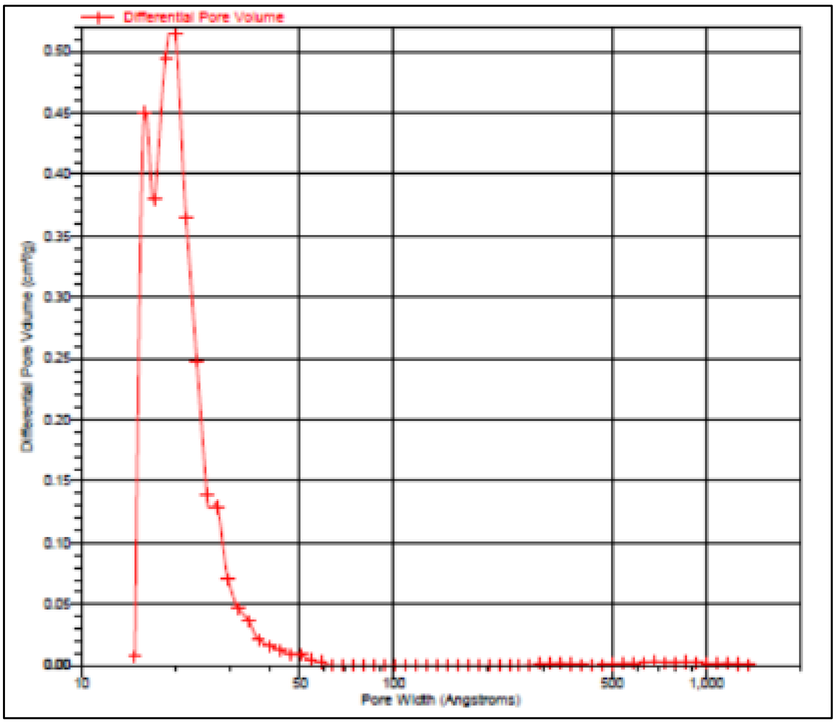

Figure 7 Volume derivative of CA-BA-H_3PO_4-40%

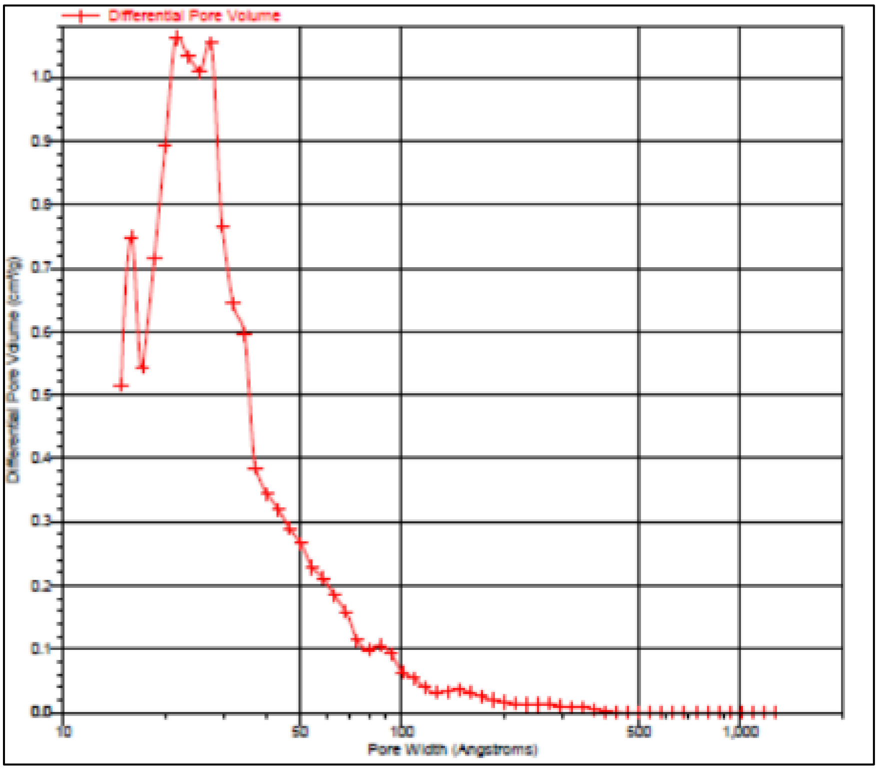

Figure 8 Volume derivative of CA-C

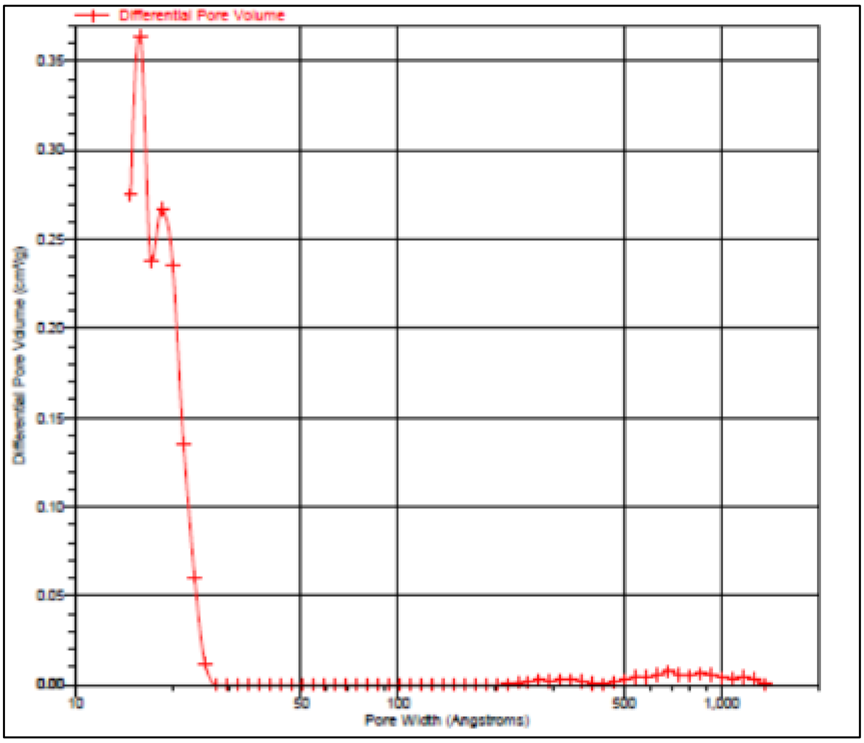

Figure 9 CA-HT-H_3PO_4-25% volume derivative

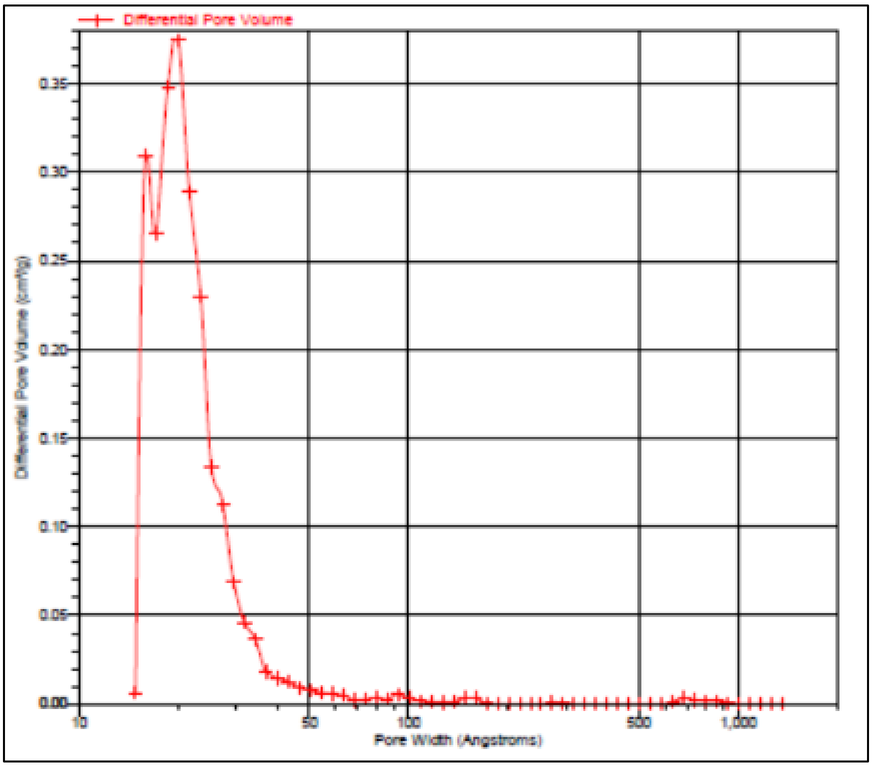

Figure 10 CA-HT-H_3PO_4-40 % volume derivative

The results of the volume distributions using the DFT method are shown in Table 2.

Table 2 Distribution of pore volumes using the DFT method

Ref. Samples	Pore volume (cm^3 g^{-1}) < 14.83 Å	Total pore volume (cm^3 g^{-1}) ≤ 1366.77 Å
CA-BA-H_3PO_4-25%	0.46474	0.56392
CA-BA-H_3PO_4-40%	0.32408	0.74954
CA-C	0.27685	0.38510
CA-HT-H_3PO_4-25%	0.19820	0.25251
CA-HT-H_3PO_4-40%	0.33989	0.41774

3.4.1. Cumulative pore volumes BJH

The cumulative pore volumes according to the BJH method are shown in Table 3.

Table 3 Cumulative pore volumes using the BJH method

Ref. Samples	Cumulative pore volume (cm^3 g^{-1} STP)	
	Adsorption	Desorption
CA-BA-H_3PO_4-25%	0.531322	0.046312
CA-BA-H_3PO_4-40%	0.560185	0.264042
CA-C	0.269688	0.172604
CA-HT-H_3PO_4-25%	0.278645	0.016532
CA-HT-H_3PO_4-40%	0.400906	0.041661

3.4.2. Average pore diameters of CAEs and CAC.

The average pore sizes are determined using the BET and BJH methods (adsorption and desorption). The results for the average pore diameters are shown in Table 4.

Table 4 Average pore diameter (Å) using the BET and BJH methods

Ref. Samples	BET Method	BJH Method	
	Adsorption	Adsorption	Desorption
CA-BA-H_3PO_4-25%	17.3617	21.331	42.400
CA-BA-H_3PO_4-40%	22.5136	27.023	41.993
CA-C	22.3516	37.995	69.847
CA-HT-H_3PO_4-25%	16.9788	20.525	52.964
CA-HT-H_3PO_4-40%	17.6995	21.537	46.316

3.4.3. DFT pore size distributions

Surface and volume pore distributions are determined by the DFT (Density Functional Theory) model.

3.5. Surface pore distributions

Figure 11 shows the isotherms of the surface distributions of CAEs and CA-C.

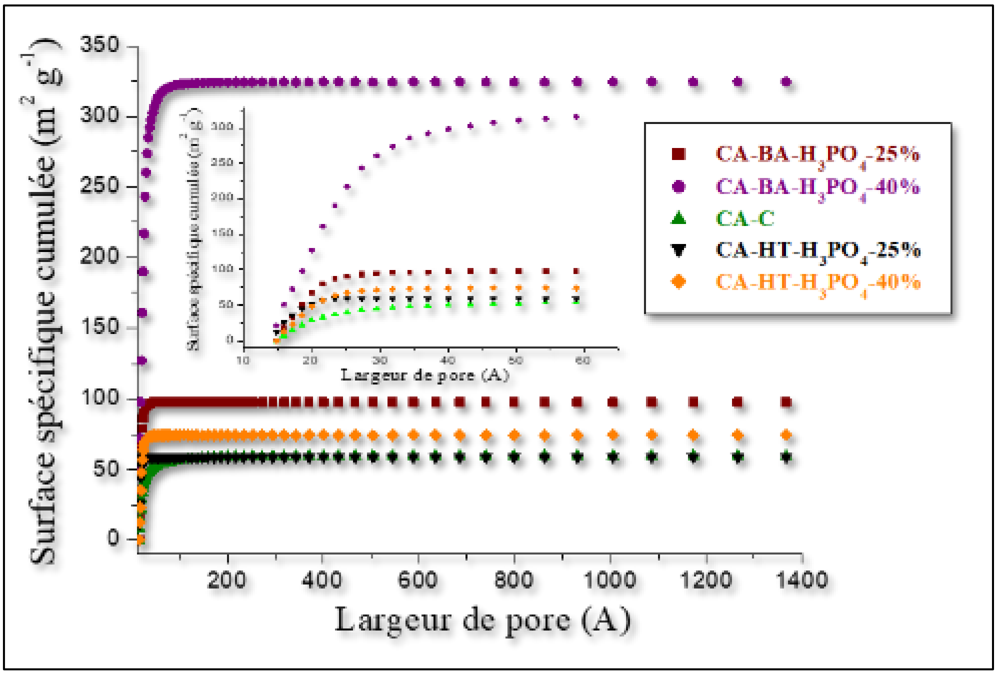

Figure 11 Surface distributions of CAEs and CAC

Figures 12, 13, 14, 15, and 16 show the derivatives of the surface distributions of the CAEs and the CA-C.

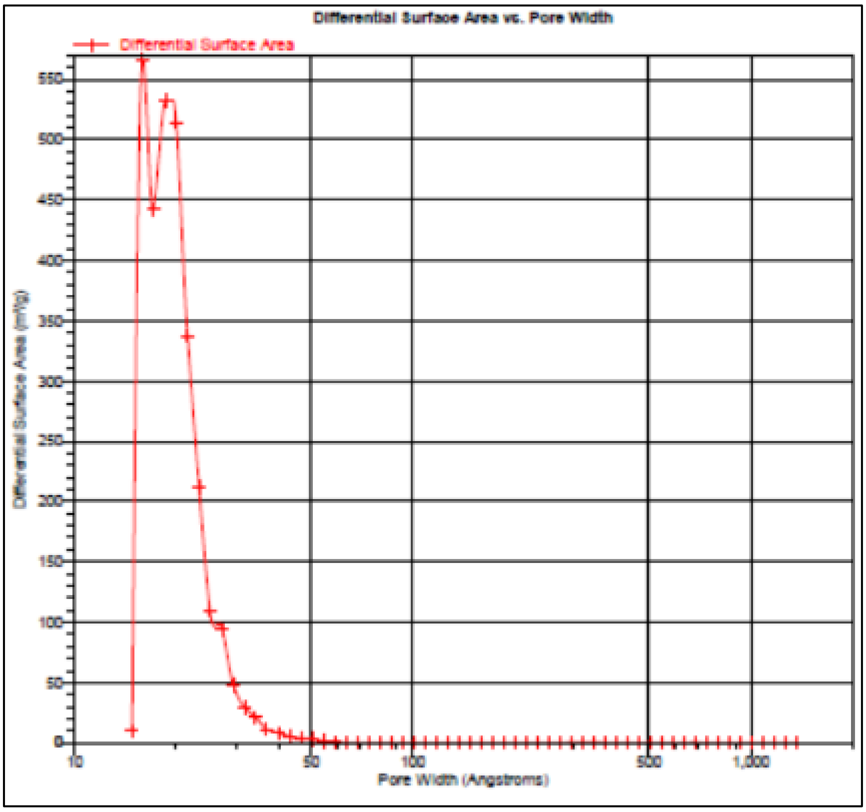

Figure 12 Surface derivative of CA-BA-H_3PO_4-25 %

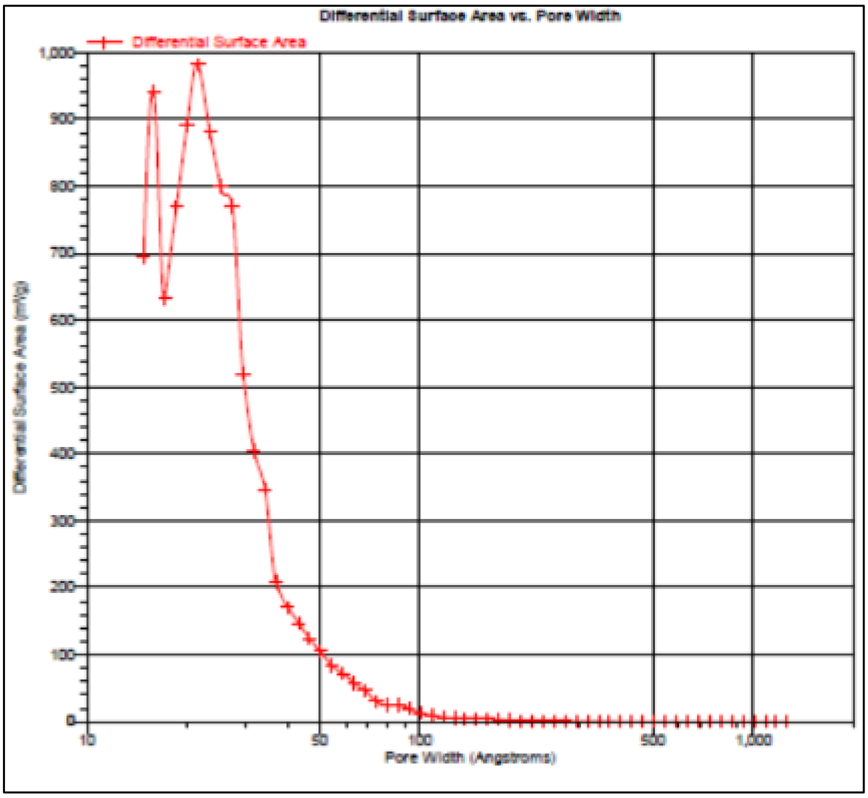

Figure 13 Surface derivative of CA-BA-H_3PO_4-40 %

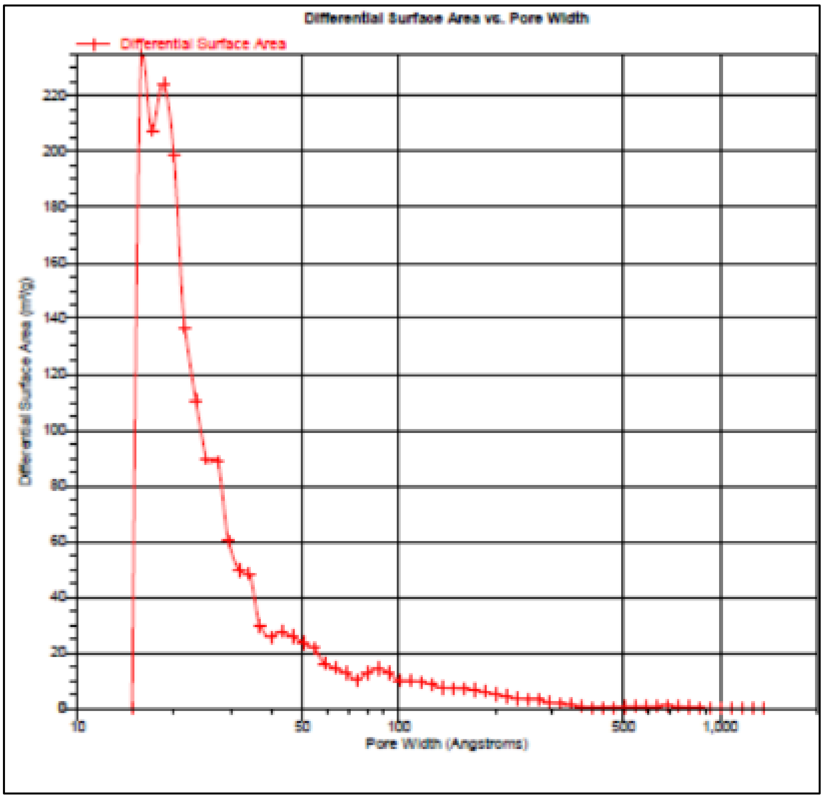

Figure 14 Surface derivative of CA-C

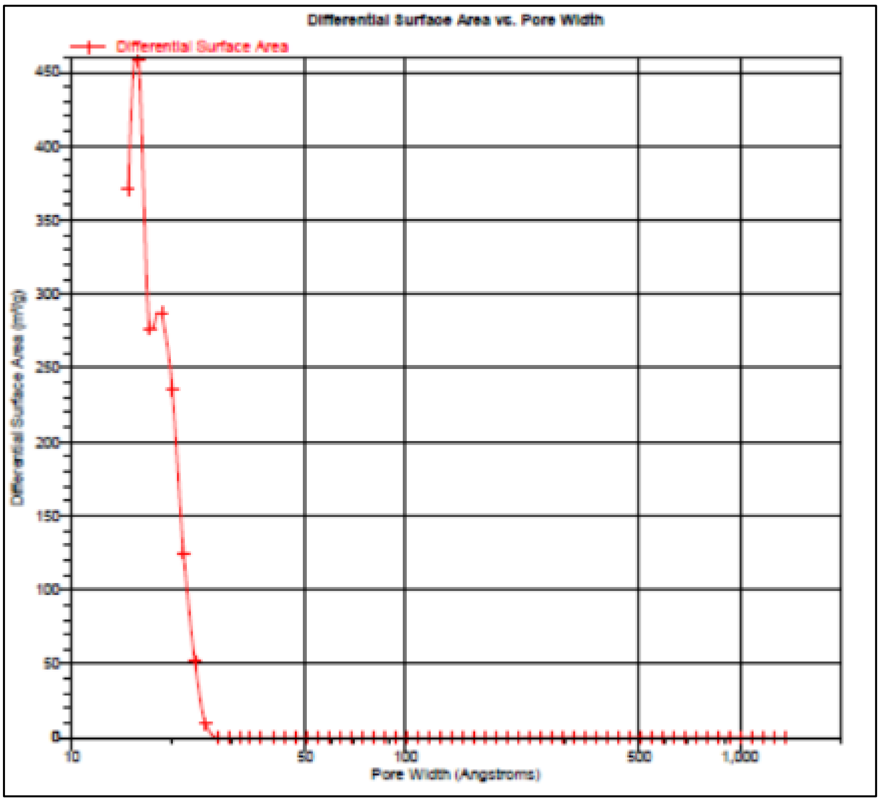

Figure 15 Surface derivative of CA-HT-H_3PO_4- 25%

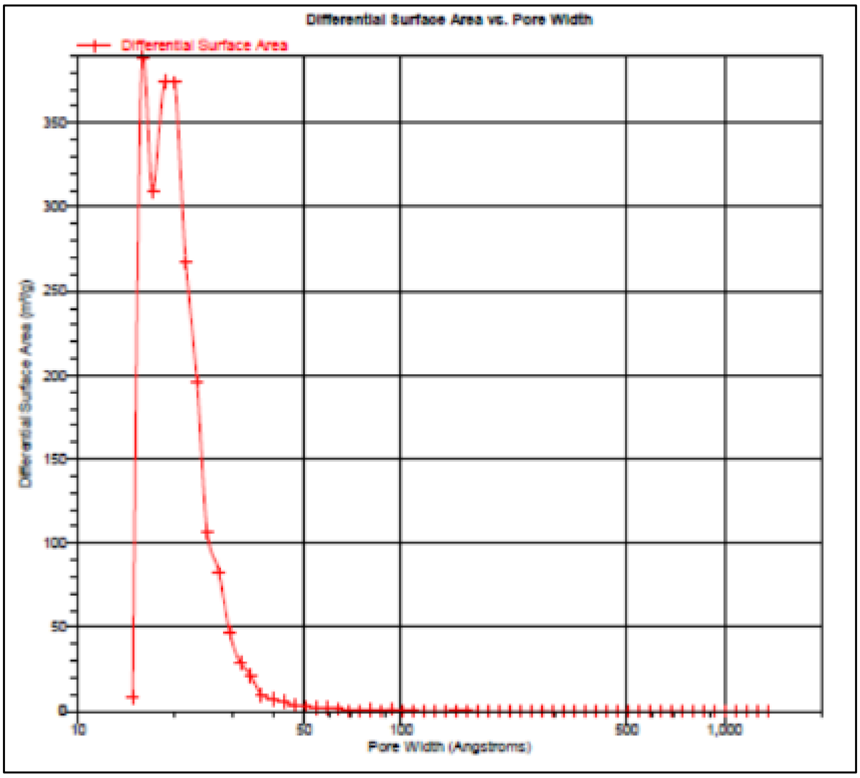

Figure 16 Surface derivative of CA-HT-H_3PO_4-40%

The results of the surface distributions are presented in Table 5.

Table 5 Distribution of pore areas using the DFT method

Ref. Samples	Pore area (m^2 g^{-1}) > 1366.77 Å	Total pore surface area (m^2 g^{-1}) ≥ 14.83 Å
CA-BA-H_3PO_4-25%	0.000	97.772
CA-BA-H_3PO_4-40%	8.063	332.591
CA-C	24.392	84.242
CA-HT-H_3PO_4-25%	0.000	58.795
CA-HT-H_3PO_4-40%	1.960	76.423

4. Discussion

Analysis of Figure 1 shows that the two diffractograms did not detect any crystallized species on the surface of the activated carbons produced. These would be characteristic of an amorphous material that does not have any detectable crystallized species on its surface [18].

Analysis of Figures 2 and 3 shows that ACEs from local biomasses have functional groups. Table 1 shows:

- Peaks attributable to carboxylic hydroxyl (O-H) groups at 3438 and 3444 cm^{-1} for CA-30 % and CA-30 % respectively;
- Signals attributable to asymmetric and symmetric C-H (2923-2853 and 2918 cm^{-1} for CA-30% and CA-30% respectively;
- Bands attributable to C=C groups (2800 and 1735, 2862 and 1731);
- Signals attributable to C=O groups (1701 and 1702 $cm^{-1;}$
- Peaks at 1493 and 1321 cm^{-1} attributable to C-O groups;
- Peaks at 1164.05 and 1189.46 cm^{-1} attributable to C-C (alkene, aliphatic, and aromatic).

The images in Figure 4 show that the biomass activation reaction created pores of different sizes (micropores, mesopores, and macropores). The existence of several types of pores after chemical activation with phosphoric acid has been observed in the literature [19].

Analysis of the results presented in Table 3 shows that:

- Adsorption: the calculated cumulative pore volumes (BJH) range from 0.269688 to 0.560185 cm^3 g^{-1} for CA-C and CA-BA-H_3PO_4-40 % respectively. They are then ranked as follows for CA-HT-H3PO4-25% (0.278645 cm^3 g^{-1}) < CA-HT-H_3PO_4-40% (0.400906 cm^3 g^{-1}) < CA-BA-H_3PO_4-25% (0.531322 cm^3 g^{-1}). The Vporeux,cul increases as a function of the percentage of the activating agent for BA and HT. Thus, the best vpoeux,cul would be obtained at 40%. The vpoeux,cul of all caes exceeds that of CA-C. All Vporeux,cul values are between 0.2 and 0.6 cm^3 g^{-1}. This confirms the microporosity phenomenon observed on the samples;
- For desorption, these Vporeux,cul values range from 0.016532 to 0.264042 cm^3 g^{-1} for CA-HT-H_3PO_4-25% and CA-BA-H_3PO_4-40%, respectively. They then follow in the following order for CA-HT-H_3PO_4-40% (0.041661 cm^3 g_{-1}) < CA-BA-H_3PO_4-25% (0.046312 cm^3 g^{-1}) < CA-C (0.172604 cm^3 g^{-1}). Apart from CA-BA-H_3PO_4-40%, all samples have values between 0.02 and 0.1 cm^3 g^{-1}, confirming the mesoporous nature of these samples. In the case of CA-BA-H_3PO_4-40%, this could be due to the external surface area developed by the latter, as it is proportional to v_{poreux}.

Analysis of the results presented in Table 4 shows that the average pore diameter values determined by the BET method range from 16.9788 to 22.5136 Å for CA-HT-H_3PO_4-25% and CA-BA-H_3PO_4-40%, respectively. This is consistent with S_{BET}, SL, and Vporeux. They then follow in the following order for CA-BA-H_3PO_4-25% (17.3617 Å) < CA-HT-H_3PO_4-40% (17.6995 Å) < CA-C (22.3516 Å). These show that the dmoy of CA-BA-H_3PO_4-25%, CA-HT-H_3PO_4-25%, and CA-HT-H_3PO_4-40% are less than 20 Å (2 nm). Thus, they correspond to the micropore size distribution. In addition, these values exceed 7 Å. This indicates that they are supermicropores. In the case of CA-C and CA-BA-H_3PO_4-40%, the dmoy values are between 20 and 500 Å. They are attributable to the mesopore size distribution. These further confirm the attribution of adsorption types. These samples are capable of adsorbing molecules of micropore and mesopore sizes. Research groups have noted that increasing the orthophosphoric acid impregnation ratio leads to a decrease in microporosity. The calculated access pore diameters, based on the desorption branch (BJH), range from 41.400 to 69.847 Å for CA-BA-H_3PO_4-40% and CA-C, respectively. For the other samples, they range from CA-BA-H_3PO_4-25% (42.400 Å) < CA-HT-H_3PO_4-40% (46.316 Å) < CA-HT-H_3PO_4-25% (52.964 Å). The diameters of the access pores obtained are essentially uniform, i.e., mesopores (20 < dmean < 500 Å). The actual pore diameters calculated from the adsorption branch range from 20.525 to 37.995 Å for CA-HT-H_3PO_4-25% and CA-C, respectively. They are followed internally by CA-BA-H_3PO_4-25% (21.331 Å) < CA-HT-H_3PO_4-40% (21.537 Å) < CA-BA-H_3PO_4-40% (27.023 Å). All these values are between 20 and 500 Å. This confirms the mesoporous nature of the access pore diameters [13-20-22].

5. Conclusion

The objectives of this work are the physical and chemical characterization of activated carbons. These studies show that:

- XRD diffractograms did not detect any crystallized species on the surface of the activated carbons;
- There are several types of pores (micropores, mesopores, and macropores). (SEM images);
- ACEs made from local biomass have developed functional groups such as carboxylic hydroxyl (O-H) groups, asymmetric and symmetric C-H groups, C=C, C=O, C-O, and C-C (alkene, aliphatic, and aromatic) groups;
- The calculated cumulative pore volumes (BJH) range from 0.269688 to 0.560185 cm^3 g-1 for CA-C and CA-BA-H_3PO_4-40% respectively;
- The Vporeux,cul increases in proportion to the percentage of activating agent for BA and HT ;
- The $V_{Poeux,cul}$ of all CAEs exceeds that of CA-C ;
- All Vporeux,cul values are between 0.2 and 0.6 cm^3 g^{-1} ;
- This confirms the microporosity phenomenon observed in the samples;
- All samples have values between 0.02 and 0.1 cm^3 g^{-1}, confirming the mesoporous nature of these samples;
- CAEs are capable of adsorbing molecules of micropore and mesopore sizes.

Compliance with ethical standards

Disclosure of conflict of interest

No conflict of interest to be disclosed.

References

[1] Gueye, M. Development of activated carbon from lignocellulosic biomass for applications in water treatment. Doctoral thesis at the International Institute for Water and the Environment (2iE), Ouagadougou/Burkina Faso OBF, 215; 2015.

[2] Ousmaila S M, Maâzou S.B. D, Abdoul Rachid C. Y, Maman Mousbahou M. A, Ibrahim N. Valorization of Balanites aegyptiaca *(L.) Del*. nut shells. and elimination of chromium in solution. Afrique SCIENCE, 14 (3), 2018, 167 – 181.

[3] Ait, S. F. Adsorption of phenol by a mixture of adsorbents (bentonite - activated carbon). Magister at the University of Boumerdèz UB, Boumerdèz-Algeria BA, 2011, 106.

[4] Siragi D. B M, Desmecht D, Hima H. I, Mamane O. S, Natatou I. Optimization of Activated Carbons Prepared from <i>Parinari macrophylla</i> Shells. MSA, vol.12, no 05, 2021, p. 207-222, doi: 10.4236/msa.2021.125014.

[5] Rabilou S M, Ousmaila S M, Zeinabou M, Mohamed M, Issa H, Maman Mousbahou M Alma, Ibrahim N. Adsorption Tests Of Ions By Raw Clays, Activated With Hydrochloric Acid And Thermally Activated At 600 °C, Followed By A Test For Depollution Of Contaminated Water. IOSR Journal of Environmental Science, Toxicology and Food Technology (IOSR-JESTFT) e-ISSN: 2319-2402, p- ISSN: 2319-2399.Volume 19, Issue 3 Ser. 1 (March 2025), PP 15-26. DOI: 10.9790/2402-1903011526.

[6] Ousmaila S.M, Maˆazou S.D.B, Mousbahou M.A.M, Ibrahim N. Valorization of the shells of Balanites aegyptiaca (L.) Del. and Hyphaene th´ebaica (L.) Mart kernels, for the development and characterization of Activated Carbons; application for the removal of chromium. ESJ 14 (2018) 195, https://doi.org/10.19044/esj.2018.v14n21p195

[7] Zeroual, S., Guerfi, K., Hazourli, S. & Charnay, C. (2011). Estimation of the heterogeneity of an oxidized activated carbon at different temperatures from the adsorption of probe molecules: Renewable Energies, 14 (4) 581-590.

[8] Avom, J., Mbadcam, J. K., Matip, M. R. L., Germain, P. (2001). Isothermal adsorption of acetic acid by plant-based carbons: AJST, Science and Engineering series, 2 (2) 1-7. DOI: http://dx.doi.org/10.4314/ajst.v2i2.44663

[9] Kheliel, O. (2014). Study of the adsorbent power of activated carbon for the denitrification of groundwater. Master's thesis at the Mohamed Khider Biskra University UMKB, Algiers-Algeria AA.

[10] Ousmaila, S.M., Adamou, Z., Ibrahim, D., & Ibrahim, N. (2016). Preparation and characterization of activated carbons based on the shells of Balanites eagyptiaca and Zizyphus mauritiana kernels: J. Soc. Ouest-Afr. Chim. 041, 59-67.

[11] Maâzou, S.D.B., Hima, I. H., Maman Mousbahou, M. A., Adamou, Z., & Ibrahim, N. (2017). Chromium removal by activated carbon prepared and characterized from the shell of the Balanites agyptiaca kernel: Int. J. Biol. Chem. Sci. 11 (6) 3050-3065. DOI: https://dx.doi.org/10.4314/ijbcs.v11i6.39.

[12] Nassim, R. (2006). Electrical and energy modeling of supercapacitors and characterization methods, Application to the cycling of a low-voltage supercapacitor module in high power: Doctoral thesis at the University of Science and Technology of Lille USTL, Lille-France LF, 201.

[13] Ousmaila, SM. Valorization of agro-food wastes for the elaboration of activated carbons; characterization and application in the depollution of wastewater loaded with chromium from the Malam Yaro Tannery of Zinder-Niger. [Doctoral thesis]. Abdou Moumouni University of Niamey. These of Doctorate Chemistry of Metals; 2019.

[14] Combere W, Arsene H. Y, Abdoulaye D, Kabore L. Removal of trivalent chromium from water by iron-exchanged zeolites and natural clays from Burkina Faso. J. Soc. West-Afr. Chem., 043, 2017, 26–30.

[15] Anwar, E. (2007). Thermal reactivity and degradation kinetics of argan wood; Application to the production of activated carbon by chemical activation with phosphoric acid: Doctoral thesis at MOHAMMED V-AGDAL UMA University, 177.

[16] Tan, I. A. W., Ahmad, A. L. & Hameed, B. H. (2008). Optimization of preparation conditions for activated carbons from coconut husk response surface methodology: Chem. Eng. J., 137, 462–470.

[17] Lua, A. C. & Yang, T. (2004). Effect of activation temperature on the textural and chemical properties of potassium hydroxide activated carbon prepared from pistachionut shell: J. Colloid Interface Sci., 274, 594-601.

[18] Girgis, B. S. & El-Hendawy, A. (2002). Porosity development in activated carbons obtained from datepits under chemical activation with phosphoric acid: Microporous Mesoporous Meter, 52, 105-117.

[19] Tchakala, I., Bawa, L. M., Djaneye-Boundjou, G., Doni, K.S., & Nambo, P. (2012). Optimization of the process for the preparation of chemically activated carbons (H3PO4) from shea cakes and cottonseed cakes: Int. J. Biol. Chem. Sci. 6 (1), 461–478. DOI: http://dx.doi.org/10.4314/ijbcs.v6i1.42

[20] Jibril, B., Houache, O., Al-Maamari, R. & Al-Rashidi, B. (2008). Effects of H3PO4 and KOH in carbonization of lignocellulosic material: Journal of Analytical and Applied Pyrolysis, 83 (2) 151-156. DOI: https://doi.org/10.1016/j.jaap.2008.07.003

[21] Bagheri, N. & Abedi, J. (2009). Preparation of high surface area activated carbon from corn by chemical activation using potassium hydroxide: Chemical Engineering Research and Design, 87 (8) 1059-1064. DOI: https://doi.org/10.1016/j.cherd.2009.02.001

[22] Sanda, M. O. Preparation of activated carbons from the shell of Balanites aegyptiaca and the shell of Zizyphys mauritiana and application of the latter in the treatment of solutions loaded with Iodine and Methylene Blue, [Master's thesis]. Abdou Moumouni University UAM, Niamey-Niger NN, 2015.